Interactions between ENSO, Monsoon and Diurnal Cycle in Rainfall Variability over Java, Indonesia

Jian-Hua Qian[1*], Andrew W. Robertson[1], Vincent Moron[2]

[1] International Research Institute for Climate and Society,
Columbia University, Palisades, New York 10964
[2] CEREGE, UMR 6635 CNRS, Aix-Marselle University,
Aix en Provence, and Institut Universitaire de France, France

Submitted on 7 October 2009 to the *Journal of the Atmospheric Sciences*

Revised 9 February 2010

*Corresponding author email: jqian@iri.columbia.edu

ABSTRACT

Using a high-resolution regional climate model RegCM3, station and satellite observations, we have studied the spatial heterogeneity of climate variability over Java Island, Indonesia. Besides the well-known anomalous dry conditions that characterize the dry and transition seasons during an El Niño year, analysis of regional model output reveals a wet mountainous south versus dry northern plains in precipitation anomalies associated with El Niño over Java during the peak rainy season. Modeling experiments indicate that this mountains-plains contrast is caused by the interaction of the El Niño-induced monsoonal wind anomalies and the island/mountain induced local diurnal cycle of winds and precipitation. During the wet season of El Niño years, anomalous southeasterly winds over the Indonesian region oppose the climatological northwesterly monsoon, thus reducing the strength of the monsoon winds over Java. This weakening is found to amplify the local diurnal cycle of land-sea breezes and mountain-valley winds, producing more rainfall over the mountains, which are located closer to the south coast than to the north coast. Therefore, the variability of the diurnal cycle associated with this local spatial asymmetry of topography is the underlying cause for the heterogeneous pattern of wet south/dry north rainfall anomalies in El Niño years. It is further shown that the mean southeasterly wind anomalies in December to February of El Niño years result from more frequent occurrence of a quiescent monsoon weather type, during which the strengthened sea-breeze and valley-breeze convergence leads to above normal rainfall over the mountains.

1. **Introduction**

Climate variability and change signals are heterogeneous at various spatial scales, especially over regions of complex topography; therefore their uncertainty (predictability) is thought to be larger (smaller) at smaller spatial scales. However, climate-related social and economic applications often require local information on climate variability and predictability in great geographical detail. On the one hand, climate variability in any local region is connected to the global environment through advection, wave propagation and teleconnections; thus, regional climate prediction has to be considered in a global context. On the other hand, although climate teleconnections are of global scale, local modulations, forced for example by fine-scale topography of terrain or land-sea contrasts, may play an important role. Therefore, understanding the role of multi-scale interaction in regional climate is critical for climate prediction and change studies and applications in weather and climate related risk management.

Java Island is the most populated island and most important industrial and agricultural region in Indonesia. It is located in the deep tropics of the southern hemisphere, at the center of the Asian-Australian monsoon region (Ramage 1968). It is zonally elongated, and slightly tilted in the northwest - southeast direction, with a central mountain range that runs the length of the island. Figure 1a shows the terrain heights based on the United States Geological Survey (USGS) 2-minute high-resolution elevation data. The central mountain range is comprised of a series of quasi-circular small volcanoes, except over West Java where the mountains are more continuously connected. In general, the central

mountain range is closer to the south coast than to the north coast, except over Central Java. Monsoonal winds and the regions of maximum rainfall associated with the inter-tropical convergence zone (ITCZ) migrate across Java annually giving rise to distinct wet season in boreal winter and dry season in boreal summer, with transition seasons in between.

At planetary scale, the Asian monsoon is driven by differential heating caused by the annual march of the sun and the spatial asymmetries of the Eurasian continent, the Pacific-Indian Oceans, and Australia (Li and Yanai 1996; Hung et al. 2004; Chang et al. 2005). At local scale of Java Island, rainfall is complicated by the underlying lower boundary forcing by highly complex island topography and land-sea contrasts (Qian 2008). For example, wind-terrain interactions produce more rainfall on the windward side of mountains (Chang et al. 2005), leading to strong modulation of rainfall patterns as the direction of the monsoonal winds reverse seasonally. The Indonesian Bureau of Meteorology, Climatology and Geophysics (BMKG) classified 293 areas of different rainfall characteristics across Indonesia, reflecting enormous complexity and heterogeneity.

Indonesian climate is strongly affected by the interannual variation of the tropical sea surface temperature (SST) in the Pacific and Indian Ocean associated with El Niño - Southern Oscillation (ENSO) and the Walker circulation (Bjerknes 1969; Zebiak 1982; Cane and Zebiak 1985; Ropelewski and Halpert 1987; Aldrian and Susanto 2003). It is well known that dry anomalies prevail in El Niño (i.e. warm ENSO) years over the

monsoonal region in Indonesia (Aldrian and Susanto 2003). However, the ENSO impact is more spatially coherent in transition season than in the wet season (Haylock and McBride 2001), and this large spatial coherence in rainfall anomalies averaged over the September–November transition season has been traced to large spatial coherence of anomalies in monsoon onset date (Moron et al. 2009). In El Niño years, the location of maximum rainfall in the Pacific basin shifts from the equatorial western Pacific toward the central-east Pacific, following the eastward displacement of warm SST anomalies (Hendon 2003; McBride et al. 2003; Juneng and Tangang 2005). Consequently, the rising branch of the Walker circulation that corresponds to the maximum rainy region shifts eastward over the warm waters, and the anomalous descending region becomes located slightly east of Indonesia (Bjerknes 1969; Wang et al. 2000; Hendon 2003); thus the low-level wind anomalies over Indonesia is easterly, in the same direction of the mean monsoonal winds in SON (southeasterlies) but becomes opposite to the mean monsoonal winds in DJF (northwesterlies) (Klein et al. 1999; Hamada et al. 2002; Giannini et al. 2007). Therefore, the El Niño increases the monsoonal wind speed in SON, but weakens the monsoonal winds in DJF in Indonesia (Bjerknes 1969; McBride et al. 2003; Juneng and Tangang 2005). Hendon (2003) proposed that the weakening of the relationship between ENSO and Indonesian rainfall from austral winter to summer is linked to this differential impact on monsoon wind speed, acting to increase evaporation and cool SSTs, suppressing rainfall during SON, while decreasing evaporative cooling during DJF.

At smaller scales, analysis of station data by Giannini et al. (2007) revealed dipolar rainfall anomalies over Java during the January–June half-year following the peak El Niño events. Moron et al. (2010) found similar spatial structures in high-resolution regional climate model (RCM) simulations, and identified associations with changes in the strength of the diurnal cycle. It was hypothesized that weak-wind weather types associated with El Niño during the peak of the rainy season cause an anomalous amplification of the diurnal cycle resulting in positive rainfall anomalies at the seasonal scale.

The objective of the present paper is to analyze this hypothesis in detail using further analyses as well as additional RCM simulations where the role of orography is removed. New evidence is presented to clearly demonstrate that interactions between ENSO, the seasonal cycle of large-scale monsoonal winds, together with the impact of the latter on the amplitude of the diurnal cycle of rainfall are key to understanding spatial patterns of seasonal rainfall anomalies over Java, and their temporal evolution between the transition and peak rainfall season. The paper is organized as follows. Section 2 details the observed and simulated data used for the analysis. Section 3 describes the background of monsoon and ENSO impacts over the broad region of Indonesia. Section 4 analyzes the fine-scale spatial pattern of anomalous rainfall over Java during ENSO years revealed in the regional model results and rain gauge data and examines the underlying multi-scale physical processes in terms of the diurnal cycle using the modeling results and observations. The connections to intraseasonal variability are documented in Sect. 5 using a weather-typing analysis. Section 6 gives further discussions on the multi-scale

physical processes and their role on the spatial and temporal rainfall variability. Conclusions are drawn in Section 7.

2. **Observed and simulated data**

A set of regional model simulations (1979-2000) were made over Indonesia with a 25km-grid resolution, in order to resolve the forcing by local mountains and coastlines, using the Abdus Salam International Centre for Theoretical Physics (ICTP) Regional Climate Model version 3 (RegCM3) (Giorgi et al. 2006; Pal et al. 2007). Its dynamical core is close to that of the hydrostatic version of the Pennsylvania State University/National Center for Atmospheric Research (PSU/NCAR) Mesoscale Model version 5 (MM5), a grid-point mesoscale model based on the primitive atmospheric equations. The vertical resolution is based on a pressure-based terrain-following sigma coordinate. There are 18 vertical levels with 6 levels in the lower atmosphere below 1.5 km height. The model was driven with observed SST within the model domain (95-130E, 12S-8N) and atmospheric data taken from the National Centers for Environmental Prediction (NCEP)/NCAR reanalysis (Kalnay et al. 1996) at the lateral boundaries are used to drive the RegCM3. The terrain of the 25km-grid RegCM3 is shown in Fig. 1b. The model roughly resolves the central mountain range along the narrow island, but individual peaks are still not well represented as compared to Fig. 1a. Note the spatial asymmetry with the mountains generally closer to the south coast than to the north coast, especially over West Java (such as the belt between the two dash lines in Fig.1a, which

will be used to derive the north-south cross section later in Figs.4 and 6) and East Java. Over Central Java, the mountains are located roughly in the middle of the island.

Satellite estimates of precipitation data cover both land and ocean, which is important for analyzing rainfall pattern across the coastlines of Java. We used a satellite-estimated rainfall dataset with a quarter-degree resolution: CMORPH (Climate Prediction Center Morphing technique) (Janowiak et al. 2005). The 3-hourly high-frequency CMORPH data can also be used to study the diurnal cycle of rainfall associated with land-sea breezes and mountain-valley winds (Qian 2008). The CMORPH data are available only recently (after 7 December 2002), therefore they cannot be used for the ENSO composite analysis directly because there are not enough ENSO events after 2002 for a statistically meaningful composite calculation. The monthly CMAP precipitation (Climate Prediction Center Merged Analysis of Precipitation, data starting in 1979) (Xie and Arkin 1996) and low-level winds (monthly and daily) from NNRP (NCEP-NCAR Reanalysis Project) were also used in the analysis, together with monthly station precipitation data over Java, obtained from the Global Historic Climatology Network (GHCN). Since there were many missing data before 1921 and after 1976 and the sparse station coverage before 1950, we only used the GHCN data in the period 1950-1975.

3. Large scale impacts of monsoon and El Niño on the climate over Java

To address the role of multi-scale processes, we first focus on large-scale processes, which are the Pacific basin scale phenomena of ENSO and the monsoon over Southeast Asia, with spatial extents in the order of magnitude of 1000 km or larger. In contrast,

local scale phenomena of land-sea and mountain-valley breezes over Java Island (~100km) will be discussed in Section 4.

Figure 2 shows the 3-monthly climatology of CMAP precipitation and NNRP low-level winds during the transition (September–November, SON), and rainy (December–February, DJF) seasons, together with their composite anomalies typical of El Niño years. The El Niño years used in the composite are the strongest six warm ENSO years during the period of 1979 to 2000 with maximum 3-monthly SST anomaly in the NINO3.4 region (5S-5N, 120-170W) larger than 1 C (1982/83, 86/87, 87/88, 91/92, 94/95, 97/98). The low-level NNRP wind divergence is depicted by the contour lines in Fig. 2.

The annual monsoon rainfall migration in the Asian-Australian region is driven by large-scale differential heating that is affected by two major factors: the incident solar radiation with the seasonal north-south march of the sun, and the planetary scale west-east land-sea contrast of the Eurasian continent and the Pacific ocean (with their different heat capacities). As a result, the area of maximum rainfall moves annually back and forth in the northwest-southeast direction; it is located near the south and east periphery of the Tibetan Plateau in boreal summer, moves southeastward in boreal fall, reaches Indonesia and Australia in boreal winter, and then moves back northwestward in boreal spring. Owing to the larger thermal inertia of the ocean compared to land, the seasonal transition from boreal summer to winter lags the change of the position of the sun by a month or two. Therefore, the average winds in SON are still in the same direction as the boreal summer monsoon of easterlies over Java. The maximum rainfall area extends across

northern Sumatra to northwest Borneo, corresponding to the ITCZ there as shown by the dash contours in Fig. 2a. Large scale low-level divergence prevails over Java in SON (solid contours), indicating stable atmospheric condition of descending motion which suppresses precipitation. In DJF, in contrast, the ITCZ is situated over Java with a maximum low-level convergence of about -2 x 10^{-6} (1/sec), indicating large scale unstable atmospheric condition of ascent favoring convection and rain. The northeasterlies of boreal winter monsoon blow from the South China Sea, turn toward the east over Sumatra and become westerlies over Java.

To examine the impact of ENSO, in Figs. 2b and 2d, we show the observed anomaly fields of CMAP precipitation, reanalysis low-level winds and horizontal divergence of the composite of El Niño years, for SON and DJF respectively. In SON of El Niño developing years (called year 0), highly spatially coherent negative precipitation anomalies prevail over the Maritime Continent. The anomalous low-level wind speed is small, but the anomalous horizontal divergence is quite large, being about 1x 10^{-6} (1/sec), almost of the same magnitude as its climatological mean in Fig. 2a. Therefore, large-scale atmospheric subsidence over Java is considerably amplified in El Niño years compared to normal years. During DJF, the easterly wind anomalies strengthen, but the magnitude of anomalous divergence decreases to only about 0.5 x 10^{-6} (1/sec), rather small compared to its mean value in Fig. 2c. The precipitation anomaly remains mostly negative in this season, but with some small pockets of positive rainfall anomaly. Because of the coarse resolution of CMAP and NNRP data (2.5 x 2.5 degrees), the dimensions of small islands, such as the width of Java (about 2 degrees or less), are of sub-grid scale. The coarse-

resolution datasets may miss local scale details, which however may be of critical concern for local users of climate risk management. In the next section, we use a high-resolution regional climate model and rain gauge and satellite observation to study this problem.

4. Local scale impacts of ENSO

4.1 A mountains/plains contrast of rainfall anomalies over Java

Figure 3 shows the RegCM3 simulated climatology of precipitation and low-level winds during SON (Fig. 3a) and DJF (Fig. 3b). The composite of the simulated anomalies in El Niño years in the two seasons are shown in panel (c) and (d), respectively. Rainfall increases substantially from the pre-monsoon transition season (SON) to the wet monsoon season (DJF). Higher rainfall is simulated over Java Island than over the surrounding seas. Qian (2008) found that this concentration of rainfall over the island is caused by the sea-breeze convergence towards the island and the valley-breeze convergence towards the mountain peaks, and further amplified by the cumulus-merger process that is more manifested in wet season than in dry and transition seasons. Therefore, the diurnal cycle of winds is very important in modulating the local precipitation in this tropical region, and we will study this problem by analyzing the regional model simulations.

The simulated composite rainfall anomalies during El Niño years (averaged values in El Niño years minus the 22-year climatology) in SON (Fig. 3c) are negative over the

whole Java Island. But the rainfall anomalies in the DJF season (Fig. 3d) show a contrast between the north and south coast over West and East Java, with the dry anomalies over the north coast and wet anomalies over the mountains near south coast, forming a north-south dipole pattern over West and East Java. Over Central Java, however, the positive anomalous rainfall is located toward the middle of the island, close to the mountain peak there. Thus, the positive rainfall anomalies during the DJF of El Niño years tend to occur over the mountainous regions of Java.

The simulated wind anomalies are smaller in SON than in DJF (Figs. 3c and 3d), similar to those of the reanalysis data shown in Figs. 2b and 2d. In El Niño years, the wind anomalies are roughly in the same direction of the climatological mean monsoonal winds of southeasterlies in SON (thus acting to slightly increase the mean southeasterly wind speed in the transition season) but opposite to the climatological northwesterly winds in DJF (thus reducing the mean northwesterly wind speed in the wet season by the cancelling effect of the southeasterly wind anomalies, Figs.2c and 2d, and Figs. 3b and 3d). Previous studies showed that this ENSO-related seasonally evolving wind differences are statistically significant (e.g., see Fig. 4 in Wang et al. 2000, Fig. 5 in Hendon 2003, and Fig. 5 in Giannini et al. 2007). As we will see later, this differential impact on monsoonal wind speed has a profound impact on the intensity of the diurnal cycle of land-sea breezes and mountain-valley winds.

Similar “dipolar” patterns of ENSO related rainfall variability over Java have previously been found in station observations by Giannini et al. (2007), and a similar

composite analysis of GHCN rain gauge data is presented in Figs. 3e and 3f for comparison with the model simulations. The period 1950-1975 was chosen based on station data coverage, with the El Niño years (1957/58, 63/64, 65/66, 68/69, 69/70, 72/73) used to calculate the composite anomalies. Consistent with the model simulations, the anomalous precipitation in SON of the El Niño-year composite is negative at every station, while the DJF station anomalies exhibit a similar dipolar structure to the RegCM3 simulated results over West and East Java (Fig. 3d), with negative and positive anomalies at northern and southern stations, respectively. Again consistent with the model, there are positive rainfall anomalies over the middle of Central Java, near the mountains there. In summary, the qualitative agreement in both seasons between observed and simulated El Niño rainfall anomalies is remarkably good in their similarity of spatial patterns.

Recently, Erasmi et al. (2009) reported that the satellite estimated normalized difference of vegetation index (NDVI) in the northern coastal plain of Java is more sensitive to the Southern Oscillation Index (SOI) but in the southern part of Java the NDVI is less sensitive to SOI due to moist conditions over the mountains (their Figs. 7 and 8), indicating potential influence on vegetation of the dipolar pattern of rainfall anomalies over Java.

4.2 Analysis of the diurnal cycle and the role of topography

By analyzing observations and regional modeling results, Qian (2008) showed the important role of the topography of island and mountains and the associated diurnal cycles of land-sea breezes and mountain-valley winds in the spatial distribution of rainfall

over Java. To illustrate the impact of topography on the climatological average rainfall distribution, Fig. 4 shows the north-south cross-section of rainfall during DJF over West Java (along the meridional belt of 106.5–108.5E) in the control run (with mountains) and in a flat-island run (in which a constant terrain height of 1.5m is used over the whole Java Island). Black bars at the bottom of Fig. 4 illustrate the simulated mountain heights in the control run over West Java (on the 25km grid). In the control run, more rainfall falls over the mountain peaks than over the northern slopes and coastal plains. This is caused by the valley-breeze convergence toward the mountain peaks, added onto the background of the island-scale sea breeze convergence during the daytime (Qian 2008). In the flat island run, however, the rainfall is quite evenly distributed across Java from the south to the north, even with slightly more rainfall near the north coast.

Figure 5 shows the 3-hourly time-bin of anomalous diurnal cycle of winds at 10 m and precipitation in DJF of El Niño years from the control run, calculated by subtracting the climatological diurnal cycle from the composite diurnal cycle in El Niño years (the daily means have also been subtracted to highlight the diurnal cycle). During the morning hours (01-13 LT, where LT denotes the Local Standard Time at Jakarta), the anomalous winds exhibit the character of land breezes diverging from Java Island toward the seas. In the afternoon (13-01 LT), the anomalous winds and rainfall are sea-breeze-like converging from the north and south coasts to the island, especially toward mountainous areas near the south coast (during the peak rainy time in the afternoon, 16-22 LT). The anomalous diurnal cycles of winds and rainfall are in phase with the climatological diurnal cycle shown in Qian (2008). Hence the diurnal cycle is strengthened in DJF of El

Niño years, especially the intensified convergence of valley winds toward the mountains that would enhance rainfall over the mountains. The modeling results indicate that the weaker monsoonal winds during DJF in El Niño years exert less interference on the local thermally driven diurnal cycle of winds and thus the strengthened land-sea breezes and mountain-valley winds change the fine-scale distribution of rainfall such that mountainous regions receive above normal rainfall.

To further examine the effect of mountains on the ENSO-related dipole pattern of rainfall anomalies over Java, Figure 6 shows a north-south cross section of the composite of rainfall anomalies in El Niño years in West Java (106.5-108.5E, between the two dash lines in Fig.1a) in the control run and flat-island run. In SON (Fig. 6a), rainfall in El Niño years is less than the climatology, i.e., rainfall anomalies are all negative from the north to the south coast, as large-scale atmosphere ascent is suppressed over the Maritime Continent in El Niño years due to the zonal displacement of the Walker circulation. The negative anomalies in the SON of El Niño years are statistically significant above 90% level of the two-tailed Student t-test. The magnitude of the rainfall anomalies is particularly large near the mountain ridge between 7-7.5S. The negative anomalies are of the same sign as those in the surrounding seas and most of Indonesia, consistent with the large-scale anomalous descent that suppresses rainfall (as indicated by Fig. 2b). The strengthened southeasterly monsoonal winds in SON in El Niño years would tend to disrupt the local thermally driven diurnal cycle of winds and thus to reduce their impact on rainfall. After the onset of wet season, with the reversal of background seasonal monsoonal winds (see Figs.2c,d; and Figs.3b,d), the reduced monsoonal wind speed in

the DJF of El Niño years has less interruption to the local diurnal cycle of winds. In this case, rainfall anomalies are positive over the southern half of West Java (over the mountains) but negative over the northern half (coastal plain), indicating that the strengthened valley breezes converge over the mountain top to produce above normal rainfall. The rainfall anomalies in Fig.6b is statistically significant (by the t-test) over the top and the southern slope of the central mountain range, and over the northern plain, in the cross section in West Java; but the rainfall anomalies are statistically insignificant over the northern slope of the mountain range, probably due to the relatively large inherent internal variability of rainfall over here during the peak of the wet season.

To demonstrate that the dipole pattern is indeed the result of mountain effects, we compare the control run with a regional model simulation in which the mountains are totally removed and replaced by a flat plain. Figs. 6c and 6d are results of the flat-island run in SON and DJF, respectively, in West Java from the south to the north along the cross section of the meridional belt of 106.5E-108.5E (Fig.1a). In both seasons, the north-south distribution of rainfall is quite even, and the rainfall anomalies in El Niño years are all slightly negative across the island. The rainfall anomalies are statistically significant in the middle and south parts of the meridional belt in West Java in SON (Fig.6c), but only significant over the Indian Ocean and Java Sea in DJF (Fig.6d). The comparison of the control run and flat-island run indicates that the north-south contrast of rainfall anomalies in El Niño years is caused by the interaction of large-scale monsoonal winds (associated with ENSO) and the diurnal cycle of winds associated with the asymmetric topography over Java (i.e., the proximity of the mountains to the south coast).

After checking the north-south cross section of rainfall in Fig. 6, we then examine the ENSO impact on the diurnal cycle of rainfall over the Java Island as a whole. Figure 7 shows the diurnal cycle (3-hourly bin) of the RegCM3 simulated precipitation and 10-m wind speed averaged over all the areas of Java Island in SON (Fig. 7a) and DJF (Fig. 7b) for the 22-year climatology, and the composite of El Niño years and La Niña years, respectively. Rain rate is large in the afternoon hours, and small in the morning hours. In SON (Fig. 7a), the 3-hourly rain rate is always smaller (larger) than the climatology throughout the day in El Niño (La Niña) years, especially in the afternoon. The diurnal cycle is thus weaker than normal in SON of El Niño years in which the anomalous winds (southeasterly) are of the same direction as the climatological winds (southeasterly) thus mean wind speed is larger than that in normal years. The rainfall anomalies in the El Niño year composite are statistically significant by the t-test. The La Niña year composite anomalies are similar in magnitude to the ones of El Niño year composite, but statistically not significant due to the larger rainfall variability over Java between the La Niña events. The climatological monsoonal winds in DJF are northwesterly, opposite to that of SON. Therefore in DJF (Fig. 7b), the mean wind speed is smaller (larger) than normal in El Niño (La Niña) years, hence the diurnal cycle is stronger (weaker) than normal in El Niño (La Niña) years. In terms of the diurnal cycle of rain rate, the differences between the El Niño year and climate are significant in the peak rainy hours in the afternoon and evening (4pm-1am). Thus, the diurnal cycle is always stronger when large-scale monsoonal winds are weaker, in both SON and DJF.

5. Relationships with daily weather types

In this section we make use of the daily weather types (WTs) constructed by Moron et al. (2010; MRQ in the following) to investigate the changes in the diurnal cycle during ENSO events in detail. This method also enables us to make use of the 3-hourly high-resolution CMORPH satellite estimates of rainfall, to indirectly analyze the ENSO impact on the diurnal cycle of rainfall, which is otherwise impossible due to the relatively short record of the CMORPH data (starting from 7 December 2002).

A *K*-means cluster analysis similar to that of Diday and Simon (1976) and Michelangeli et al. (1995) was used to classify weather regimes based on the unfiltered NNRP daily 850 hPa circulation field over the Maritime Continent region (MRQ). Daily winds are standardized to zero mean and unit variance using the long-term August-February climatology and then pre-filtered by the Empirical Orthogonal Function analysis retaining the 9 leading principle components, accounting for 75% of the total variance (MRQ). Initially, a prescribed number (*k*) of clusters are specified and daily observations are agglomerated around centroids chosen from random seeds. Then, iterative clustering calculations are carried out to minimize the sum, over all clusters, of the within-cluster spread, to finally reach the clusters that localize relatively high concentrations in data distribution in the atmospheric phase space. The multi-year daily time sequence of weather types describes a systematic monsoonal evolution, as well as the variability at seasonal and interannual time scales (MRQ).

Five daily weather types (WT 1 to 5) were identified by MRQ from the *K*-means cluster analysis in August–February over the Maritime Continent region, over the period 1979 to 2007, representing daily weather regimes in the pre-monsoon and wet season. These results are zoomed over an area around Java using composites in Fig. 8 in terms of 850 hPa winds (1979–2007), as well as the CMORPH rainfall averaged over all days for each WT during the available data period 2003–2007. Both variables are plotted without the mean subtracted. The two relatively dry weather types over Java, WT1 and WT2, are characterized by southeasterly winds in the lower atmosphere over Java; these correspond to the pre-monsoon and transition phases of the seasonal evolution. The three rainy weather types, WT3, WT4, and WT5, have westerly winds over Java, corresponding to wet season monsoonal winds, with much more rainfall over Java. Because wind speeds across monsoonal Indonesia south of the equator are small in WT4, it was referred to as the quiescent monsoon by MRQ. Note that while rainfall over the region surrounding Java is small in WT4 compared to WT3 and WT5, the rainfall over Java Island itself is appreciable. This is consistent with our previous analysis that local land-sea breezes are more prominent when the background monsoon is weak. In WT3 and WT5, strong westerly winds and relatively heavy rainfall cover most of the Indonesian region, but rainfall over Java Island is smaller than that in WT4.

Figure 9 shows the frequency of the five weather types averaged in all years, and in El Niño and La Niña years, during the pre-monsoon (SON, Fig. 9a) and wet monsoon (DJF, Fig. 9b) season, respectively. The sum of the frequencies of the five WTs for each season equals to 100%, for example, the sum of blank bars in Fig. 9a is 100%. The

climatological seasonal evolution of WTs is such that WT1, WT2 and WT3 dominate in SON, then WT3, WT4, and WT5 prevail in DJF (see MRQ). The impact of ENSO on WT frequency is clearly marked in both seasons. During SON of El Niño events, the dry southeasterly WT2 becomes more frequent relative to the less frequent wet westerly weather type WT3, while during DJF the quiescent WT4 becomes much more prevalent at the expense of the strong westerly WT3 and WT5, as discussed in MRQ.

Next we analyze the diurnal cycles of rainfall in these five weather types to elucidate the role of ENSO in modulating the local rainfall distribution. The satellite-estimated precipitation of CMORPH data (Dec 2002–present) is too short for ENSO composite analysis, but there are many days of different weather types for a composite analysis based on the weather types. Figure 10a shows the diurnal cycle of CMORPH rainfall for the five WTs averaged over the whole area of Java Island. The rain rate and the diurnal cycle are much smaller in the dry weather types (WT1 and 2) than the wet ones (WT3, 4, and 5). Note that the diurnal cycle of rainfall over Java Island is strongest for WT4, the quiescent monsoon type. While the regional-scale rainfall over Indonesia as a whole is largest in the strong monsoon types WT3 and WT5 (Fig. 8), the quiescent WT4 produces the most rainfall over Java Island (Fig. 10a). Figure 10b shows the diurnal cycle of the RegCM3 simulated rainfall for the five WTs, in which WT4 also has the slightly stronger diurnal cycle than WT3 and WT5, being consistent to the satellite data shown in Fig. 10a. However, the differences in simulated diurnal cycles between the WTs are much smaller than in the CMORPH when averaged over the whole of Java. Also note that the simulated diurnal cycle shows the early timing with somewhat flat peaks, probably due to the

discrepancies in the cumulus scheme such as the insufficient representation of the entrainment/detrainment rate of clouds (Del Genio and Wu 2010).

As discussed earlier, the diurnal cycle over the mountains should be stronger than that over the plains, because of the combined effect of in-phase land-sea and mountain-valley breezes. Figure 10c and 10d show the diurnal cycle of rainfall over the mountainous regions over Java (those areas with elevation higher than 250 meters). Indeed, the diurnal cycles over the mountains are stronger than the corresponding ones averaged over the whole island (Fig. 10a,b), particularly in the regional model. It is also apparent that more rainfall is received over the mountainous regions during quiescent large-scale weather conditions (WT4) than during the strong monsoon weather types WT3 and WT5.

During DJF of El Niño years, the northwesterly monsoon is weaker than normal, and the quiescent monsoon WT4 is the dominant weather type (Fig. 9b, with over 60% of frequency of occurrence by this weather type alone in the wet season), in which the intensified diurnal cycle of winds converge more moisture toward the mountainous region and produce more abundant rainfall over there (Fig. 10c,d). Thus, we attribute the increase in rainfall over mountains at the expense of the plains during the wet season of El Niño years to the increased frequency of large-scale quiescent winds (WT4) that promote the diurnal cycle.

6. Discussion on multi-scale physical processes

A new source of spatio-temporal variability of ENSO-induced rainfall anomalies over Java is identified, associated with multi-scale processes of ENSO, the seasonal monsoon winds, subseasonal weather types, and local-scale diurnal sea/valley breeze circulations. In the pre-monsoon and transition season SON, large scale vertical motion associated with the Walker Circulation and the local scale diurnal cycle of winds work in concert to either enhance rainfall (in La Niña years) or suppress rainfall (in El Niño years) over the mountainous Java Island. For instance, in El Niño years, the large-scale sinking associated with the Walker circulation suppresses rainfall over the Maritime Continent, and meanwhile the strengthened southeasterly monsoonal winds act to weaken the sea-breeze and valley-breeze convergence that also reduce rainfall over Java Island, especially over the mountains. Therefore, in SON, the magnitude of rainfall anomalies is quite large in both El Niño and La Niña years with largest deviation from the climatology reaches up to 5 mm/day during afternoon hours.

Unlike that in SON, the large-scale vertical motion and local diurnal cycle during the monsoon season in DJF work against each other to affect rainfall over Java. In DJF of El Niño years, although large-scale anomalous descent associated with the Walker circulation suppresses rainfall over Java, the strengthened sea-breeze and valley-breeze convergence (due to the weaker than normal monsoon wind speed) enhances rainfall over Java. The results show that the local effect prevails over the large-scale effect, especially over the mountains. The maximum rain rate in the DJF of El Niño years is larger than the

climatology by about 5 mm/day in the afternoon, and the positive anomalies prolonged toward late evening. But in the DJF of La Niña years, the diurnal cycle is only slightly weakened as compared to the climatology, indicating an asymmetry that the El Niño impacts are usually stronger than the La Niña impacts (Fig. 7).

Note that the ENSO impact on the averaged wet season rainfall over Java Island is somewhat opposite to the overall large-scale regional impact over the Maritime Continent shown in Fig. 2d. The averaged rainfall is above (below) normal in El Niño (La Niña) years over Java Island in the afternoon hours. These ENSO-induced rainfall anomalies are mostly contributed by the more prominent impact over the mountainous regions, namely the contrasting mountains/plains pattern of rainfall anomalies addressed by this paper. The rainfall is spatially redistributed, with more rainfall over the mountains, and less rainfall over the plains and valleys, because of the intensified diurnal cycle of winds in El Niño years.

On sub-seasonal timescales, the weather typing analysis reveals that the major difference caused by ENSO during SON is the difference of frequencies between the dry and wet weather types, in that less (more) wet WT3 in SON in El Niño (La Niña) years, caused negative (positive) rainfall anomalies over the whole Java Island in SON. While in DJF, the ENSO impacts are the difference of frequencies between the three wet weather types. The most prominent feature is that the quiescent weak monsoon WT4 strongly prevails in El Niño years that exerts less influence on the thermally driven local diurnal cycle of land-sea breezes and mountain-valley winds, which converge to the

mountainous regions, which are near the south coast over West and East Java but about in the middle in Central Java, forming the wet mountains versus dry plains and valleys heterogeneous pattern of rainfall anomalies in El Niño years.

The north coast and the valley regions over Java (where most people live) share the same sign of rainfall anomalies as most areas of Indonesia in El Niño years, consistent with the large-scale descending and stabilizing effect of the Walker circulation. It is probably how El Niño is generally perceived to cause below-normal rainfall over Java. However, the rainfall over Java Island as a whole does not necessarily decrease (in fact, it even slightly increases) in El Niño years, as shown in the station rainfall, CMORPH satellite data and modeling results (more frequent WT4, which produce more rainfall over mountains of Java Island). The less rainfall over the plains and valleys is compensated by the excessive rainfall garnered over the mountains.

It should be noted that the above phenomenon of heterogeneous precipitation anomalies revealed by the composite analysis of RCM and station and satellite data is a general or canonical feature of El Niño's impact over Java. However, every El Niño event is somewhat different according to the historical record. Therefore, whether the contrasting pattern of rainfall anomalies is realized in each El Niño event depends on the specific SST structure of that event. Also, we used RCM with a grid size of 25km, so the sub-grid scale forcings, such as small scale hills and curved coastlines which may cause further complexity, are still not fully resolved in the model (as indicated by the difference between Fig. 1a and 1b). However, since the intensity of the diurnal cycle is inversely

proportional to the ambient large-scale monsoonal wind speed, it is perceivable that even at smaller spatial scales (< 25km), this variability of diurnal land-sea and mountain-valley winds will generally make flat places drier and high mountain areas wetter in the wet season in El Niño years, and vice versa in La Niña years. The above argument may also be valid for other islands with similar climate and topography, such as Sumatra, Sulawesi, and Timor, which warrants further investigation.

The seasonally-dependent mechanism for ENSO-induced rainfall anomalies over Java put forward in this paper can be compared to previous hypotheses for the decrease in spatial coherence (and seasonal predictability) from SON to DJF. Hendon (2003) hypothesized that El Niño rainfall anomalies lose coherence after monsoon onset because (large-scale) ENSO-induced wind speed anomalies decrease sharply when the seasonal winds reverse, progressing from a reinforcing to a canceling of the easterly anomalies and (seasonally dependent) mean field. In Hendon (2003)'s argument, the sharp drop in wind speed during El Niño reduces evaporation, allowing negative SST anomalies around Indonesia to warm, offsetting large-scale anomalous subsidence impact of El Niño over Indonesia. Giannini et al. (2007) argued that the tropical ocean-atmosphere equilibrates to ENSO, and ENSO itself begins to decay, its direct influence diminishes, and regional features associated with the delayed response to ENSO become more prominent. In the current study, we demonstrated that the diurnal cycle is essential for the ENSO and monsoon influences on the local fine-scale rainfall distribution over Java.

7. Conclusion

The interannual rainfall variability over Java has been analyzed using observation and regional climate modeling experiments. The mountain-plain dipolar pattern of rainfall anomalies associated with ENSO that is revealed in both modeling and station data and its mechanism is analyzed from the perspective of multi-scale physical processes: the Pacific Ocean basin-scale interannual climate variability of ENSO modulates of the annual and seasonal monsoon intensity over Indonesia, and the monsoon intensity affect the diurnal cycle of land-sea breezes over the Java Island and the mountain-valley winds within the island. The key is the inverse relationship between the intensity of the monsoonal wind speed and the amplitude of the diurnal-cycle. The weakened northwesterly monsoon (by the more frequent occurrence of the daily quiescent weather regime) in the DJF of warm ENSO years causes the strengthened land-sea and mountain-valley breezes, which helps to retain negative rainfall anomalies over the coastal plains but acts to enhance low-level moisture convergence towards the central mountain range and produce more rainfall over the mountains. This is found to be the mechanism for the wetter mountains versus drier plains dipolar pattern of rainfall anomalies in the peak rainy season over the Java Island associated with El Niño.

Acknowledgments: We wish to thank Filippo Giorgi, Xunqiang Bi and other members in the Abdus Salam ICTP, the developers of RegCM3. We also thank Alessandra Giannini for discussions. We are grateful for the constructive comments of three anonymous reviewers that helped to improve the paper greatly. The IRI represents a cooperative agreement between the U.S. National Oceanic and Atmospheric Administration (NOAA) Office of Global Programs and Columbia University. The paper is funded by a grant/corporative agreement from the NOAA NA05OAR4311004. The views expressed herein are those of the authors and do not necessarily reflect the views of NOAA or any of its sub-agencies.

REFERENCES

Aldrian, E., and R.D. Susanto, 2003: Identification of three dominant rainfall regions within Indonesia and their relationship to sea surface temperature. *Int. J. Climatol.*, **23**, 1435-1452.

Bjerknes, J., 1969: Atmospheric teleconnections from the Equatorial Pacific. *Mon. Wea. Rev*., **97**, 163-172.

Cane, M.A., and S.E. Zebiak, 1985: A theory for El Niño and Southern Oscillation. *Science*, **228**, 1085-1087.

Chang, C.P., Z. Wang, J. McBride, and C.-H. Liu, 2005: Annual cycle of Southeast Asia-Maritime Continent rainfall and asymmetric monsoon transition. *J. Clim.*, **18**, 287-301.

Del Genio, A.D., and J. Wu, 2010: The role of entrainment in the diurnal cycle of continental convection. *J. Clim.*, In press.

Erasmi, S., P. Propastin, and M. Kappas, 2009: Spatial pattern of NDVI variation over Indonesia, and their relationship to ENSO warm events during the period 1982-2006. *J. Clim.*, **22**, 6612-6623.

Giannini, A., A.W. Robertson, and J.-H. Qian, 2007: A role for tropical tropospheric temperature adjustment to El Niño – Southern Oscillation in the seasonality of monsoonal Indonesia precipitation predictability. *J. Geophys. Res.*, **112**, D16110, doi: 10.1029/2007JD008519.

Giorgi, F., J.S. Pal, X. Bi, L. Sloan, N. Elguindi, and F. Solmon, 2006: Introduction to the TAC special issue: The RegCNET network. *Theor. Appl. Climatol.*, **86**, 1-4.

Hamada, J.I., M.D. Yamanaka, J. Matsumoto, S. Fukao, P.A. Winarso, T. Sribimawati, 2002: Spatial and temporal variations of the rainy season over Indonesia and their link to ENSO. *J. Meterol. Soc. Jap.*, **80**, 285-310.

Hendon, H.H., 2003: Indonesian rainfall variability: impacts of ENSO and local air-sea interaction. *J. Clim.*, **16**, 1775-1790.

Haylock, M., and J. McBride,2001: Spatial coherence and predictability of Indonesian wet season rainfall. *J. Clim.*, **14**, 3882-3887.

Hung, C.-W., X. Liu, and M. Yanai, 2004: Symmetry and Asymmetry of the Asian and Australian summer monsoons. *J. Clim.*, **17**, 2413-2426.

Janowiak, J.E., V.E. Kousky, and R.J. Joyce, 2005: Diurnal cycle of precipitation determined from the CMORPH high spatial and temporal resolution global precipitation analyses. *J. Geophys. Res.*, **110**, D23105, doi:10.1029/2005JD006156.

Juneng, L., and F.T. Tangang, 2005: Evolution of ENSO-related rainfall anomalies in Southeast Asia region and its relationship with atmosphere-ocean variations in Indo-Pacific sector. *Int. J. Climatol.*, **25**, 337-350.

Kalnay, E. and Coauthors,1996: The NCEP/NCAR 40-year reanalysis project. *Bull. Amer. Meteor. Soc.*, **77**, 437-471.

Klein, S.A., B.J. Soden, N.G. Lau, 1999: Remote sea surface temperature variations during ENSO: evidence for a tropical atmospheric bridge. *J. Clim.*, **12**, 917-932.

Li, C., and M. Yanai, 1996: The onset and interannual variability of the Asian summer monsoon in relation to land-sea thermal contrast. *J. Clim.*, **9**, 358-375.

McBride, J.L., M.R. Haylock, and N. Nicholls, 2003: Relationships between the Maritime continent heat source and the El Niño – Southern Oscillation phenomena. *J. Clim.*, **16**, 2905-2914.

Michelangeli, P.A., B. Lagras, and R. Vautard, 1995 : Weather regimes : recurrence and quasi-stationarity. *J. Atmos. Sci.*, **52**, 1237-1256.

Moron, V., A.W. Robertson, and R. Boer, 2009: Spatial coherence and seasonal predictability of monsoon onset over Indonesia, *J. Clim.*, **22**, 840-850.

Moron, V., A.W. Robertson, and J.-H. Qian, 2010: Local versus large-scale characteristics of monsoon onset and post-onset rainfall over Indonesia. *Climate Dyn.*, **34**, 281-299.

Pal, J.S. and Coauthors, 2007: Regional climate modeling for the developing world: The ICTP RegCM3 and RegCNET. *Bull. Am. Meteorol. Soc.*, **88**, 1395-1409.

Qian, J.-H., 2008: Why precipitation is mostly concentrated over islands in the Maritime Continent. *J. Atmos. Sci.*, **65**, 1428-1441.

Ramage, C.S.,1968: Role of a tropical “maritime continent” in the atmospheric circulation. *Mon. Wea. Rev.*, **96**, 365-370.

Ropelewski, C.F., and M.S. Halpert, 1987: Global and regional scale precipitation patterns associated with the El Niño/Southern Oscillation. *Mon. Wea. Rev.*, **115**, 1606-1626.

Wang, B., R. Wu, and X. Fu, 2000: Pacific-East Asia teleconnection: How does ENSO affect Asian climate? *J. Clim.*, **13**, 1517-1536.

Xie, P., and P.A. Arkin,1996: Analysis of global monthly precipitation using gauge observations, satellite estimates, and numerical model predictions. *J. Clim.*, **9**, 840-858.

Zebiak, S.E., 1982: A simple atmospheric model of relevance to El Niño. *J. Atmos. Sci.*, 3**9**, 2017-2027.

Figure Captions

Figure 1: Terrain heights (meters) over Java Indonesia in (a) the USGS observation, and (b) RegCM3 modeled terrain with 25km-grids. The two vertical dash lines denote the longitudes of 106.5 E and 108.5 E. The meridional belt will be used for cross-section analyses in Figs. 4 and 6.

Figure 2: Climatology (1979-2000) and (El Niño - climatology) composites of CMAP precipitation (mm/day; shaded), and NNRP winds (vector) and divergence (red contours with interval of 0.5×10^{-6} 1/sec, divergence is thin solid, convergence thin dash, zero-curves thick solid) at 925 hPa, for SON (a,b), and DJF (c,d). El Niño years used for the composite are: 1982/83, 86/87, 87/88, 91/92, 94/95, 97/98. El Niño developing years are denoted by (0).

Figure 3: Climatology of the NCEP/NCAR reanalysis driving RegCM3 simulated rainfall (mm/day) in SON (a) and DJF (b) over Java Indonesia. Composite analysis of (El Niño - climatology) of the RegCM3 results of anomalous precipitation (mm/day, shaded) and low-level winds (m/s, vector) at σ =0.995 are in (c) for SON, and (d) for DJF. El Niño years used for the composite analysis in this time period are 1982/83, 86/87, 87/88, 91/92, 94/95, and 97/98. Composite station rainfall anomalies in El Niño years based on the GHCN dataset are in (e) for SON and (f) for DJF. GHCN data of 1950-1975 are used. The El Niño years used for the composite analysis are 1957/58, 63/64, 65/66, 68/69, 69/70, 72/73.

Figure 4: Climatology of RegCM3 (1979-2002) precipitation (mm/day, shaded) across Java Island along the meridional belt of 106.5-108.5E, averaged in December to February for the control run with mountains (solid) and the flat-island run (dash). Black bars at the bottom illustrate terrain heights along the meridional belt. West Java latitudes range between 6.2S to 7.7S along the meridional belt.

Figure 5: The El Niño minus climatology composite of diurnal cycle of the NNRP-driving RegCM3 simulated precipitation (mm/day, shaded), and winds (m/s, vector) at 10m in DJF. Daily means are subtracted to highlight the diurnal cycle. (El Niño years: 1982/83, 86/87, 87/88, 91/92, 94/95, 97/98).

Figure 6: The north-south cross section of the RegCM3 simulated seasonal precipitation (mm/day): climatology (solid), El Niño year composite (long dash), El Niño minus climatology (short dash, where the differences statistically significant above 90% level of confidence of the student t-test are shown by thick dash lines and crosses), along the meridional belt (106.5E-108.5E) in West Java (the extend of the island, 6.2S-7.7S, is illustrated by a thick line at the bottom of each panel). Panels (a) and (b) are for SON and DJF in the mountainous control run; panels (c) and (d) are for SON and DJF in the flat-island run. The six El Niño years in the simulation period used in the composite calculation are: 1982/83, 1986/87, 1987/88, 1991/92, 1994/95, and 1997/98.

Figure 7: Diurnal cycle of RegCM3 simulated rainfall (mm/day, thick curves) and wind speed (m/s, thin curves) over the whole area of Java Island in SON (a) and DJF (b) for climatology (solid), El Niño (EN) year composite (long dash), and La Niña (LN) year composite (short dash). Rainfall differences between ENSO years and climatology that are statistically significant above the 90% level of confidence of the student t-test are shown by thick lines and crosses. Wind speeds at 10 m are plotted with the same scale with unit of m/s. “LT” denotes the local standard time at Jakarta Indonesia.

Figure 8: Composites of CMORPH (2004-2007) precipitation for weather types WT1-5 (mm/day, shaded) and NNRP reanalysis winds at 850 hPa (m/s).

Figure 9: Frequencies of five weather types WT1 to WT5, in all years (blank left bars), El Niño years (black middle bars), and La Niña years (grey right bars) in SON (a) and DJF (b) season, respectively.

Figure 10: Diurnal cycles of the CMORPH and RegCM3 rainfall (mm/day) over the whole Java Island (a, b) and over mountainous regions (terrain elevation higher than 250 m) (c, d) for weather types: WT1 (solid), WT2 (dot dash), WT3 (short dash), WT4 (long dash) and WT5 (dot). “LT” denotes the local standard time at Jakarta Indonesia.

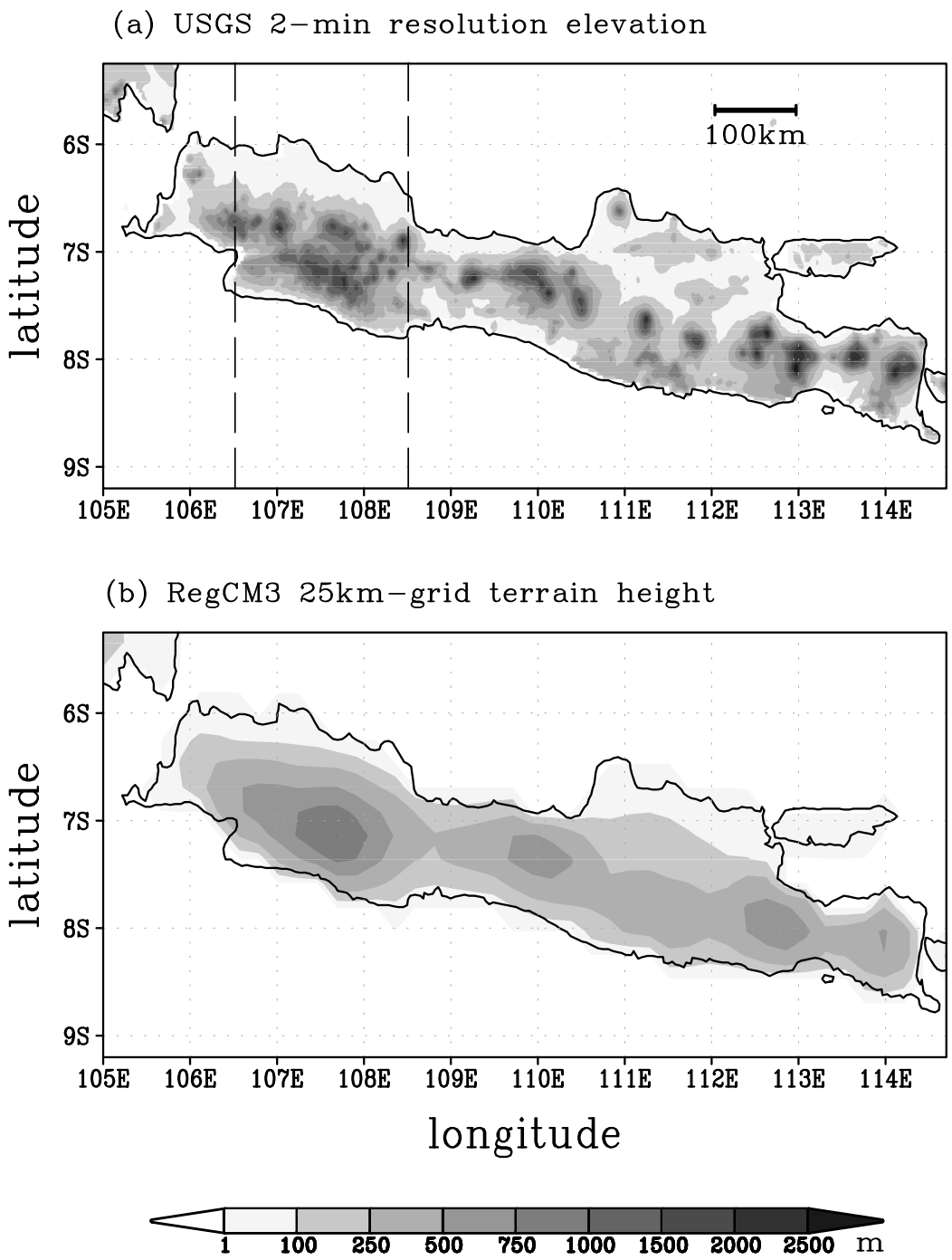

Fig.1 Terrain heights (meter) over Java, (a) USGS observation, (b) RegCM3 25km−grid.
The two vertical dash lines denote the longitudes of 106.5E and 108.5E.
The meridional belt in West Java will be used for cross−section analyses in Figs. 4 and 6.

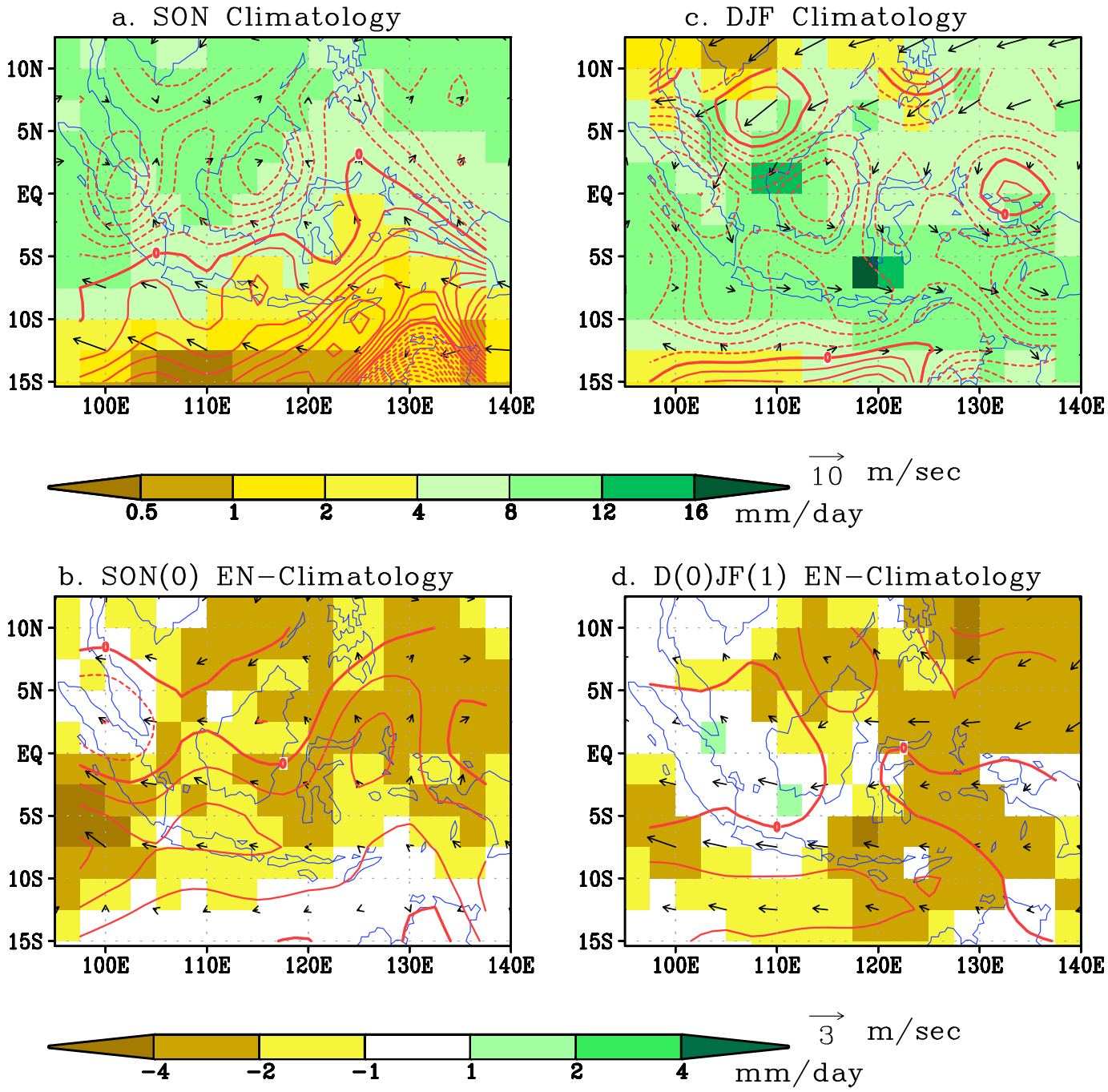

Fig.2 Climatology (1979−2000) and (El Nino − climatology) composite of CMAP precipitation (mm/day; shaded), and NNRP winds (vector) and divergence (red contours with interval of 0.5e−6/sec, divergence is thin solid, convergence thin dash, zero−curves thick solid) at 925hPa, for SON (a, b), and DJF (c, d). El Nino years used for the composite are: 82/83, 86/87, 87/88, 91/92, 94/95, 97/98. El Nino developing years are denoted by (0).

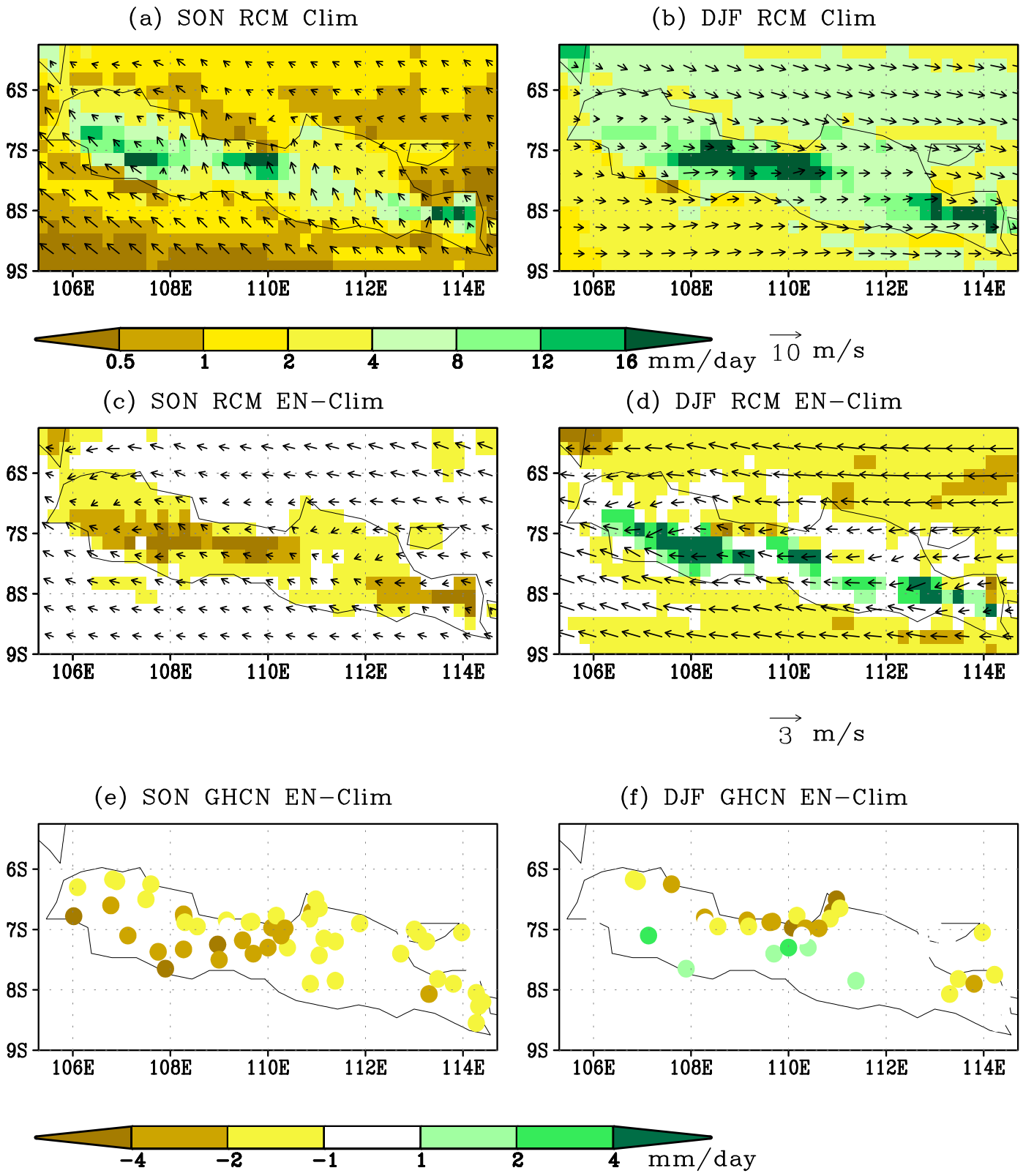

Fig.3 Climatology of NCEP−reanalysis−driving RegCM3 simulated rain (mm/day) and low level winds (m/s) (at sigma=0.995) in SON (a) and DJF (b); (El Nino − climatology) composite of RegCM3 simulated rain (mm/day) and winds (m/s) in SON (c) and DJF (d); and (El Nino − climatology) composite of GHCN guage rain (mm/day) in SON (e) and DJF (f).

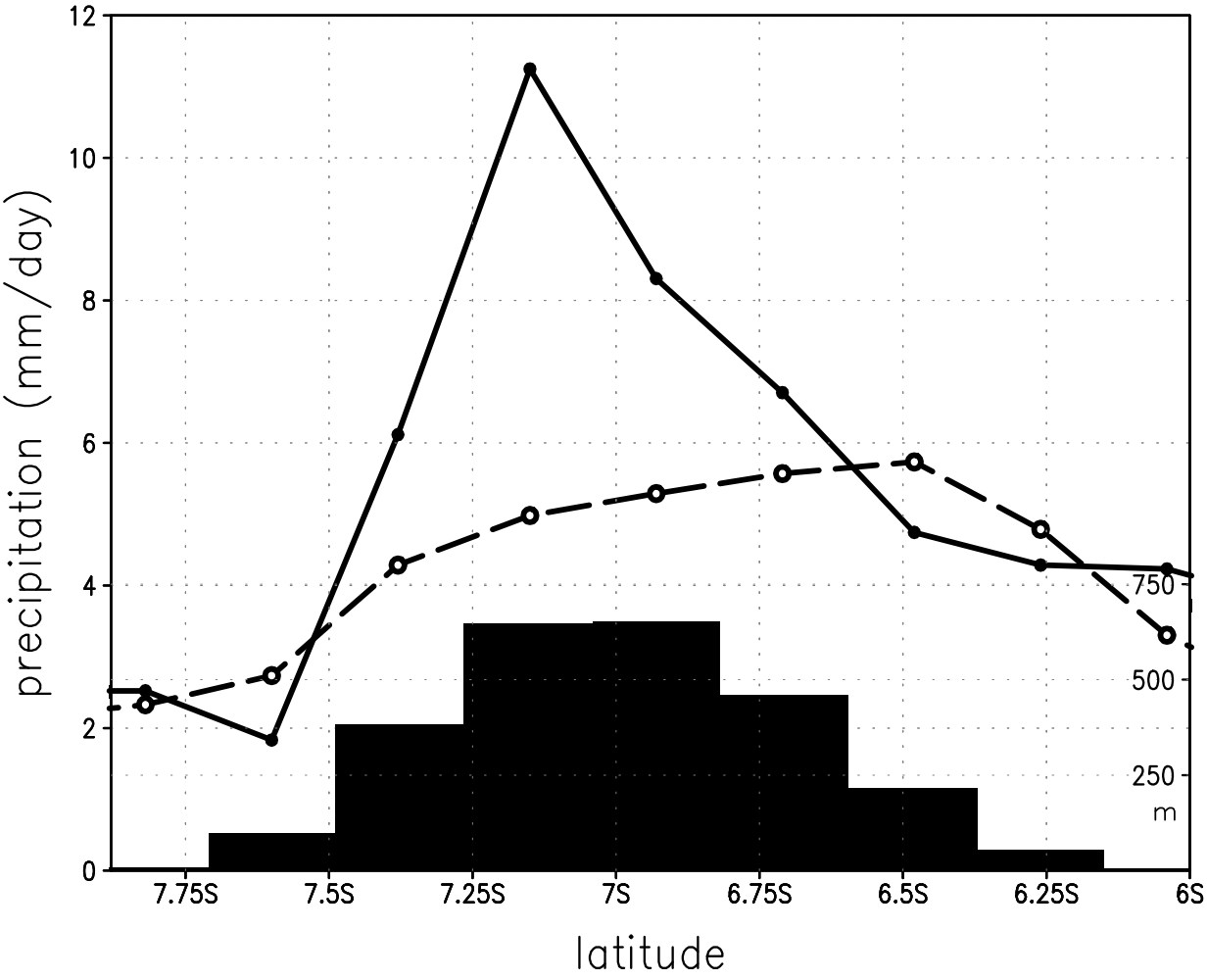

Fig.4 Climatology of RegCM25 (1979–2002) precipitation (mm/day; shaded) across Java Island along the meridional belt of 106.5–108.5E, averaged in December to February for the control run with mountains (solid) and the flat–island run (dash). Terrain heights (m, right axis) along the meridional belt are illustrated by black bars at the bottom. Java Island ranges averagely from 6.2S to 7.7S along this belt.

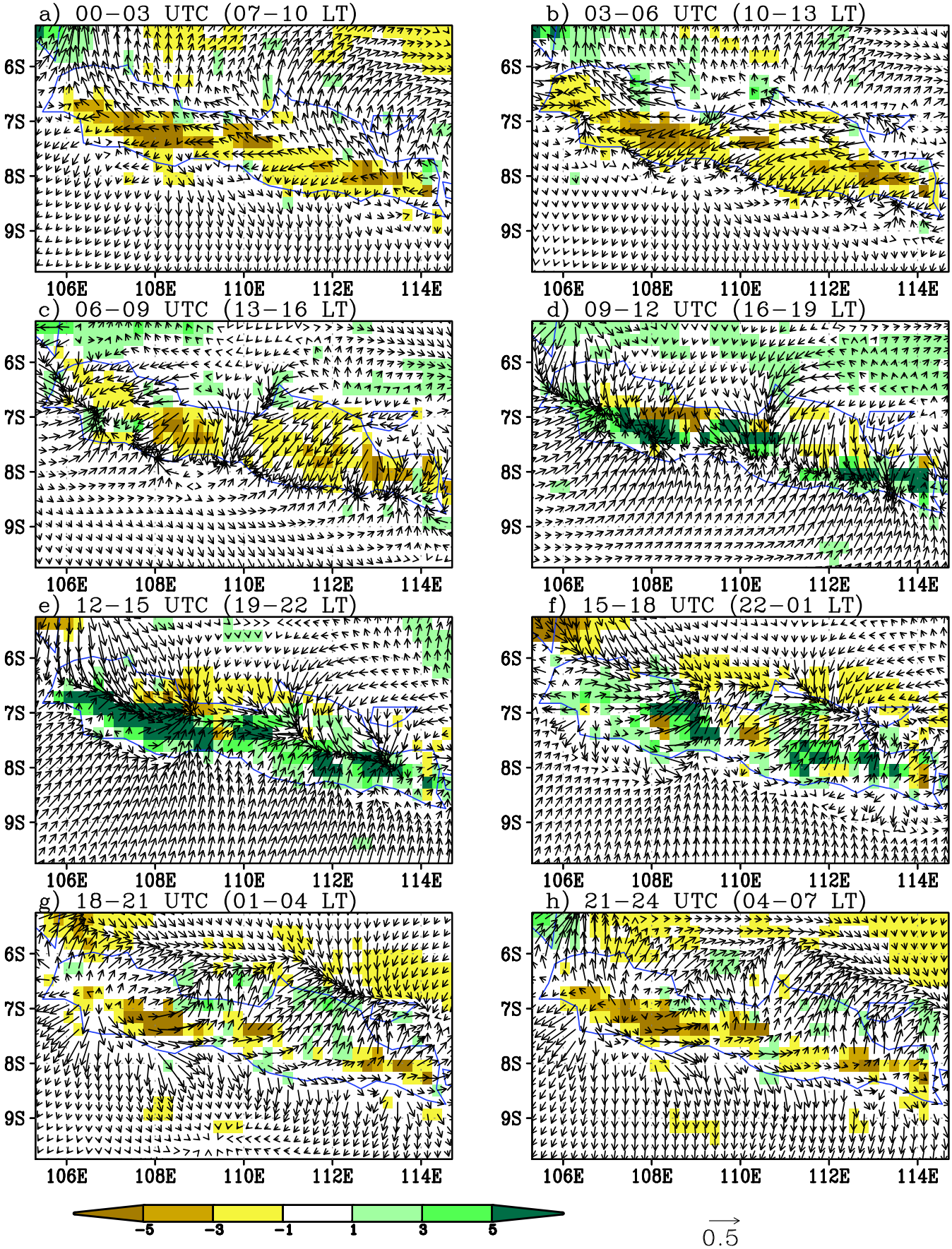

Fig.5 (El Nino − climatology) composites of diurnal cycle of NNRP−driving RegCM3 precipitation (mm/day; shaded), and winds (m/s, vector) at 10 m [D(0)JF(1)].
(Res: 25km; El Nino years: 82/83, 86/87, 87/88, 91/92, 94/95, 97/98) indo−simulation
(Difference of anomalies, with daily means of El Nino years and climatology removed)

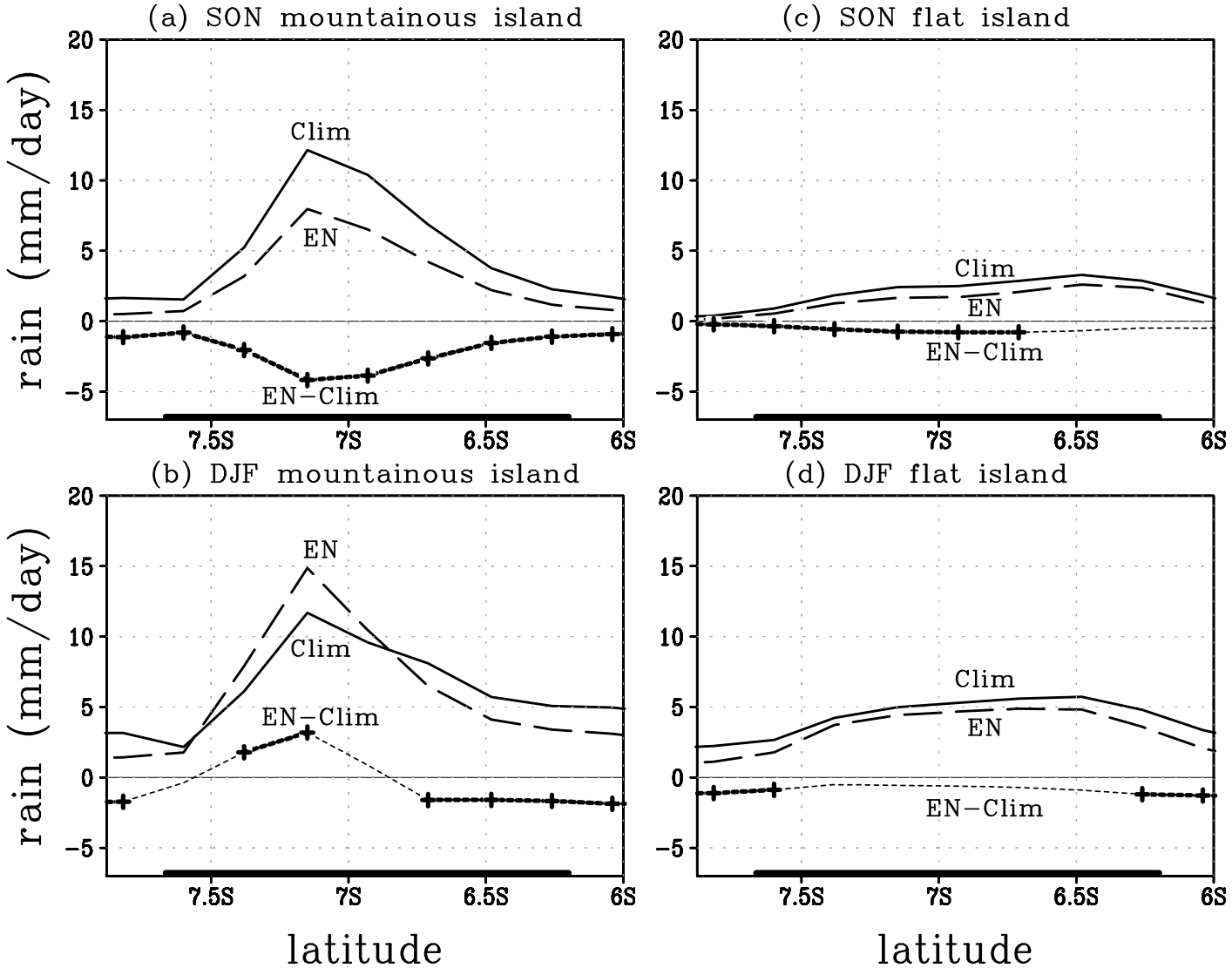

Fig.6 North−south cross section of the RegCM3 simulated seasonal precipitation (mm/day): climatology (solid), El Nino year composite (long dash), and EL Nino munus climatology (short dash, where differences significant above 90% level of the t−test are shown by thick dash lines and crosses), along the meridional belt of (106.5E−108.5E) in West Java, the extent of which (6.2S−7.7S) is illustrated by a thick line at the bottom of each panel. Panels (a) and (b): SON and DJF in the mountainous control run; panels (c) and (d): SON and DJF in the flat island run. The six El Nino years used in the composite calculation are: 1982/83, 1986/87, 1987/88, 1991/92, 1994/95, and 1997/98.

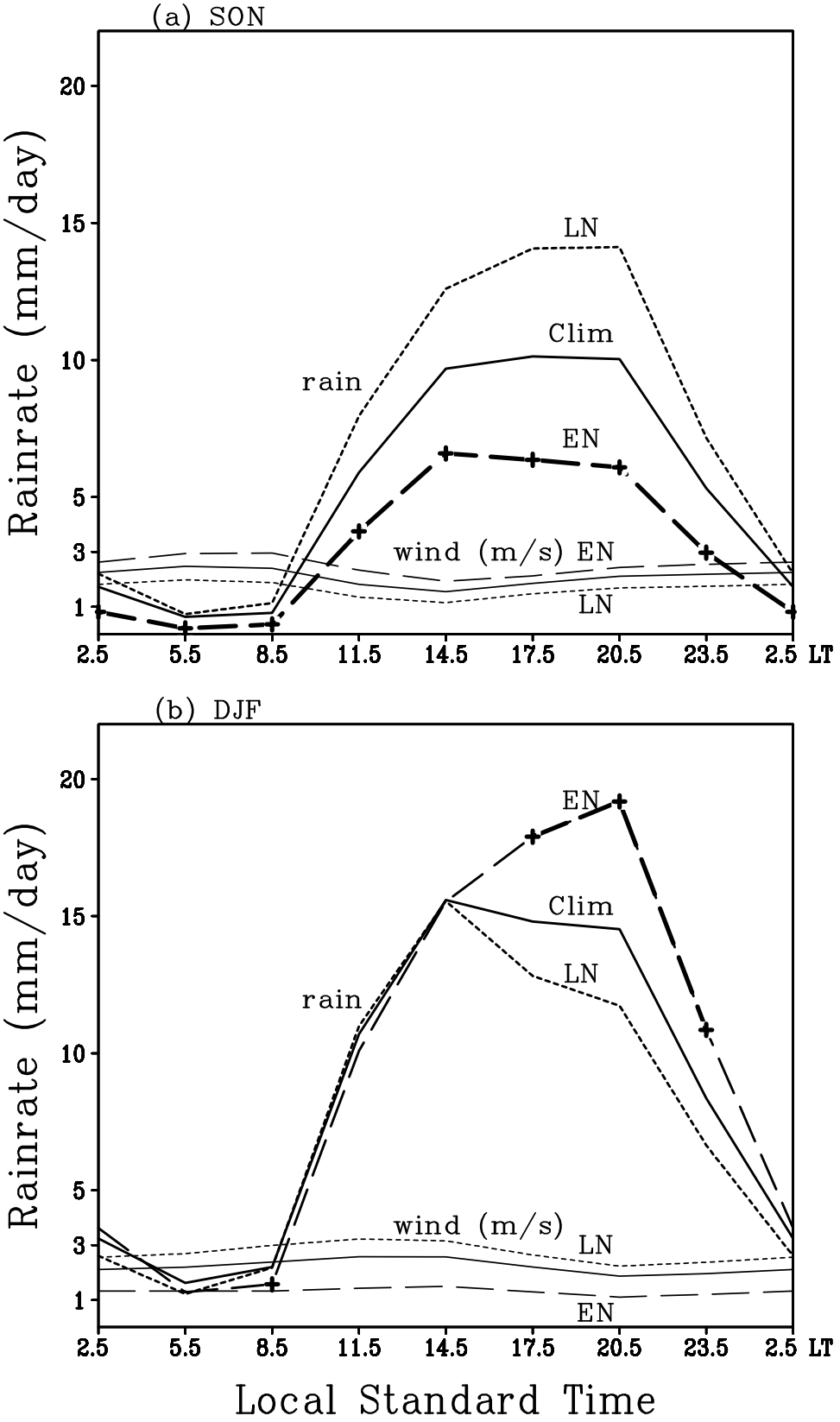

Fig.7 Diurnal cycles of RegCM3 rainfall (thick, mm/day) and wind speed (thin, m/s) over the whole area of Java Island in SON (a) and DJF (b) for climatology (solid), El Nino year (EN) composite (long dash), and La Nina year (LN) composite (short dash). Rainfall differences between ENSO years and climatology that are significant above 90% level of t−test are shown by thick lines and crosses. Wind speeds at 10 m are plotted with the same scale, but with unit m/s. "LT" denotes the local standard time at Jakarta.

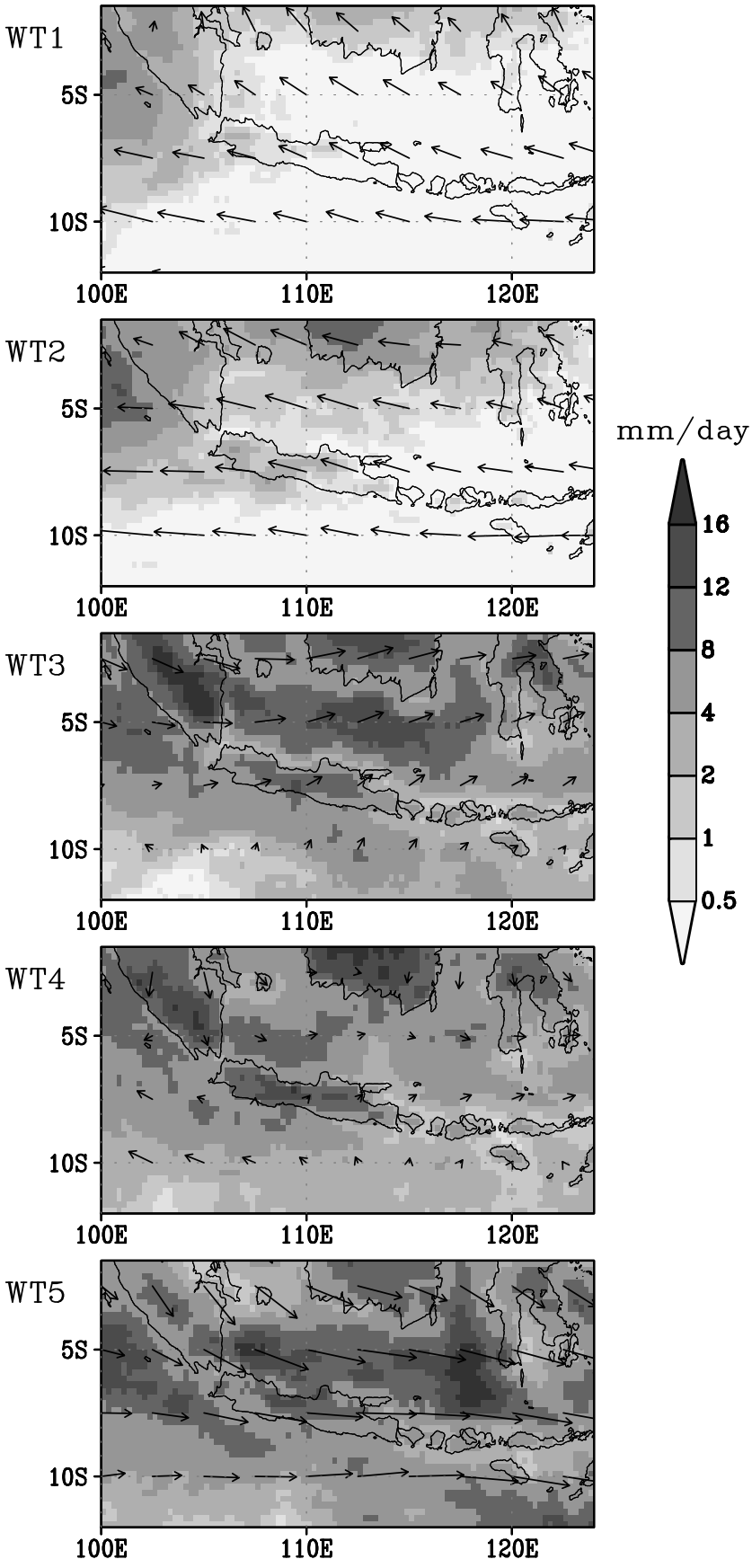

Fig.8 Composites of CMORPH (2004–2007) precipitation WT1–5 (mm/day; shaded) and NNRP reanalysis winds at 850 hpa (m/s).

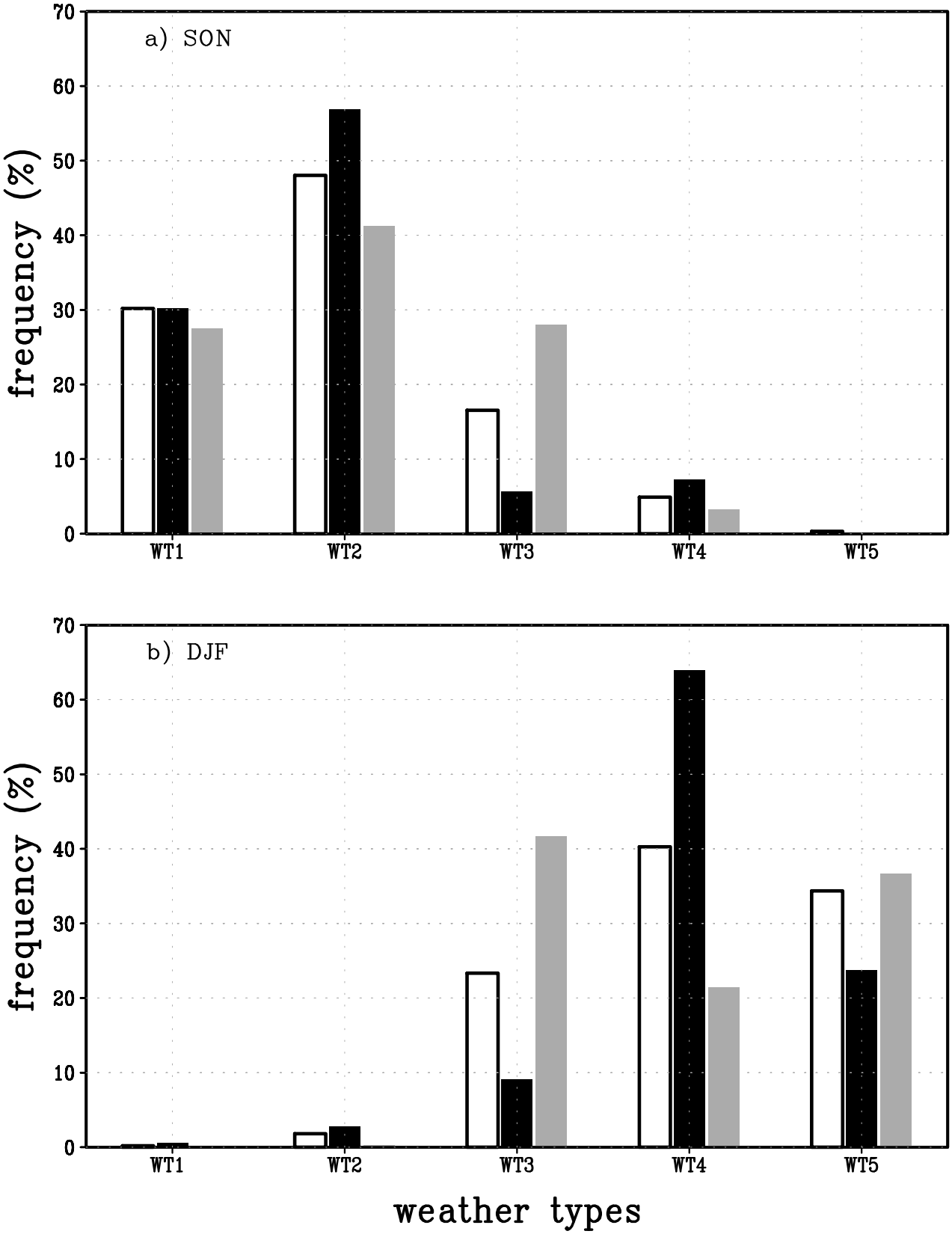

Fig.9 Frequencies of five weather types, WT1 to WT5, in all years (blank left bar), El Nino years (black middle bar), and La Nina years (gray right bar) in the SON and DJF season, respectively.

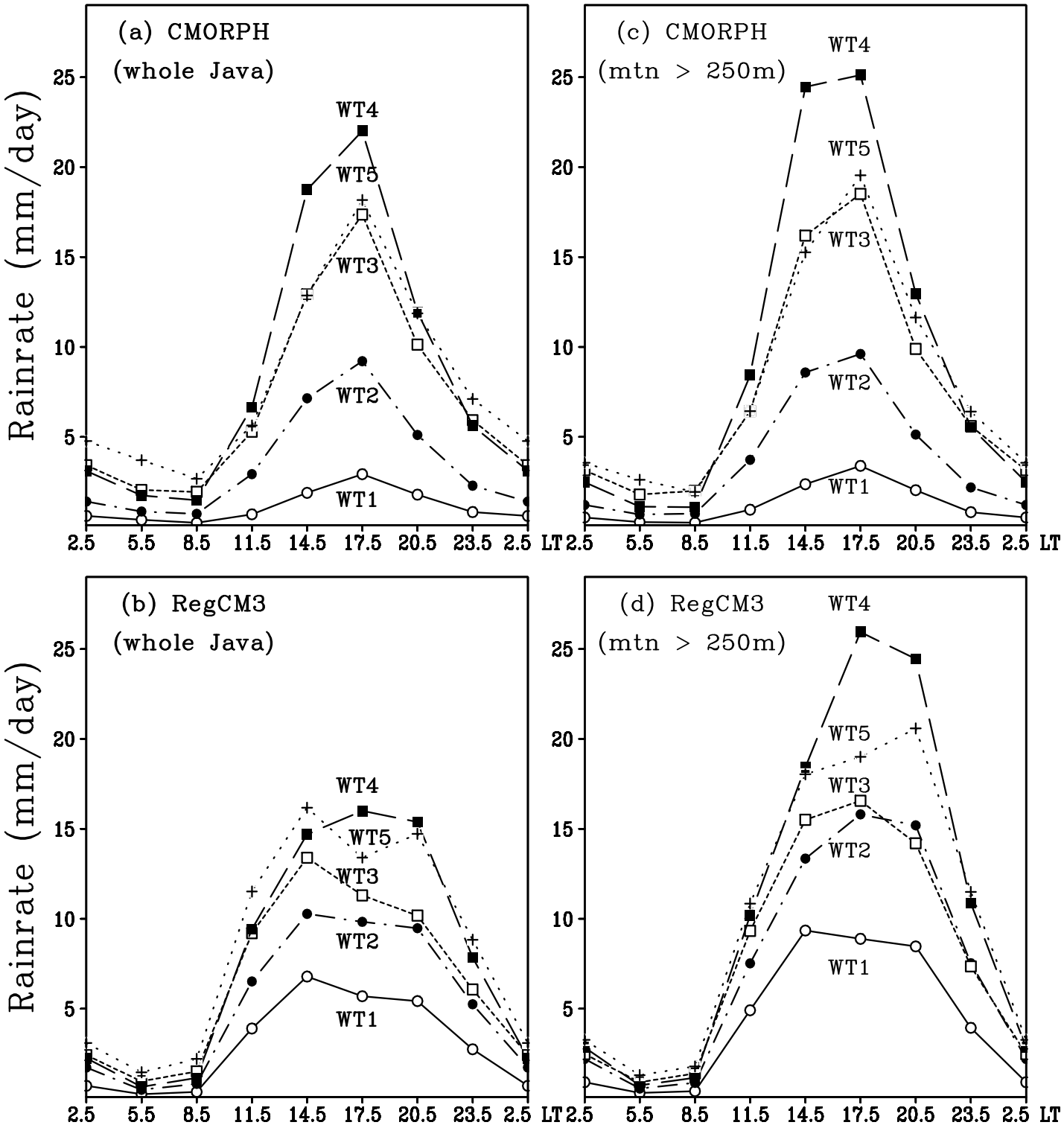

Fig.10 Diurnal cycles of CMORPH and RegCM3 rainfall (mm/day) over the whole area of Java Island (a, b) and over mountainous regions (terrain height > 250 m) (c, d) for weather types: WT1 (solid), WT2 (dot dash), WT3 (short dash), WT4 (long dash), WT5 (dot). "LT" denotes the local standard time at Jakarta Indonesia.